A semianalytical model of fractured horizontal well with hydraulic fracture network in shale gas reservoir for pressure transient analysis

Qianchen Cui[1], Yulong Zhao[1,*], Liehui Zhang[1], Man Chen[2], Shangjun Gao[2], Zhangxing Chen[3]

[1]State Key Laboratory of Oil and Gas Reservoir Geology and Exploitation, Southwest Petroleum University, Chengdu 610500, PR China

[2]Sichuan Changning Natural Gas Development Co., Ltd., Chengdu 610056, PR China

[3]Department of Chemical and Petroleum Engineering, University of Calgary, Calgary, T2N 1N4, Canada

*Corresponding Author: Dr. Yulong Zhao. Email: swpuzhao@swpu.edu.cn; ORCID: 0000-0002-5621-6420

Appendix A. Definition of the Parameter Dimensionless Rules

The dimensionless parameters related to length or distance are defined as follows:

$$\Theta_D = \begin{cases} \dfrac{\Theta}{L_{HF}}, (\Theta = r, R_e, \delta, \zeta, h_t, h_H, h_c^{'}, w_F, l_{HW}, l_{HF}, l_{BF}, l_{SF}, x, y, a_e, b_e) \\ \dfrac{\Theta}{R_m}, (\Theta = r_m, R_m) \end{cases} \tag{A-1}$$

where L_{HF} is the half-length of the HF, m.

The other dimensionless parameters are defined as follows:

$$\eta_{mD} = \frac{\eta_m}{\eta_f}, \eta_{oD} = \frac{\eta_o}{\eta_f}, \eta_{FD} = \frac{\eta_F}{\eta_f}, \eta_{fD} = 1 \tag{A-2}$$

$$\begin{cases} m_{\zeta D} = \dfrac{\pi k_f h_t T_{SC}}{q_{SC} p_{SC} T}(m_i - m_\zeta) \\ q_D = \dfrac{p_{SC} T}{\pi k_f h_t T_{SC}(m_i - m_f)} \end{cases}, (\zeta = m, o, f, HF) \tag{A-3}$$

$$t_D = \frac{\eta_f}{L_{HF}^2} t_a \tag{A-4}$$

$$F_{CD} = \frac{k_{HF} w_F}{k_f L_{HF}} \tag{A-5}$$

Appendix B. Derivation of the Seepage Equations of the Matrix System

For the shale matrix particles

Using Laplace transformation, the dimensionless seepage equation of the gas flow in the matrix block and

boundary conditions is as follows:

$$\begin{cases} \dfrac{\partial^2 \overline{m}_{mD}}{\partial r_{mD}^2} + \dfrac{2}{r_{mD}} \dfrac{\partial \overline{m}_{mD}}{\partial r_{mD}} - \dfrac{s}{\eta_{mD}} \overline{m}_{mD} = 0 \\ \lim\limits_{r_{mD} \to 0} \left(r_{mD}^2 \dfrac{\partial \overline{m}_{mD}}{\partial r_{mD}} \right) = 0 \\ \overline{m}_{mD} \big|_{r_{mD} = R_{mD}} = \overline{m}_{fD}(r_D, s) \end{cases} \tag{B-1}$$

To solve the second-order partial differential equations of spherical coordinates as Eq. (B-1), apply the following substitution:

$$\overline{m}_{mD} = \frac{\overline{w}_{mD}}{r_{mD}} \tag{B-2}$$

By using Eq. (B-2), Eq. (B-1) can be written as follows:

$$\begin{cases} \dfrac{\partial^2 \overline{w}_{mD}}{\partial r_{mD}^2} - \dfrac{s}{\eta_{mD}} \overline{w}_{mD} = 0 \\ \lim\limits_{r_{mD} \to 0} \overline{w}_{mD} = 0 \\ \overline{w}_{mD} \big|_{r_{mD} = R_{mD}} = \overline{w}_{fD} \end{cases} \tag{B-3}$$

The solution of Eq. (B-3) is:

$$\overline{w}_{mD} = \frac{\sinh\left(\sqrt{u_{mD}} r_{mD}\right)}{\sinh\left(\sqrt{u_{mD}} R_{mD}\right)} \overline{w}_{fD} \tag{B-4}$$

Then, substituting Eq. (B-2) into Eq. (B-4) can get the Eq. (23) in this paper.

For the microfracture of shale matrix

The dimensionless equation of gas flow in micro-fracture in the Laplace domain is as follows:

$$\nabla^2 \overline{m}_{fD} + \frac{2}{h_{fD}} \frac{k_m}{k_f} \frac{\partial \overline{m}_{mD}}{\partial r_{mD}} \bigg|_{r_m = R_m} - \frac{s}{\eta_{fD}} \overline{m}_{fD} = 0 \tag{B-5}$$

Based on the Eq. (9) and the dimensionless parameter defend in Appendix A, can get:

$$\begin{cases} \nabla^2 \overline{m}_{fD} - f_f(s) \overline{m}_{fD} = 0 \\ f_f(s) = \dfrac{s}{\eta_{fD}} - \dfrac{2}{h_{fD}} \dfrac{k_m}{k_f} \left[\dfrac{1}{\tanh\left(\sqrt{u_m(s)} R_{mD}\right)} - \dfrac{1}{R_{mD}} \right] \end{cases} \tag{B-6}$$

For micro-fracture in OFNR under the assumption of a closed circular boundary, the pressure solution is given as follows:

$$\overline{m}_{fD,i} = \tilde{\overline{q}}_{D,i} \int_{-L_{FD,i}}^{+L_{FD,i}} \mathrm{K}_0[\sqrt{f_f} r_D]\mathrm{d}r_D \tag{B-7}$$

For microfracture in OFNR with a rectangular closed boundary, the pressure solution is given by:

$$\overline{m}_{fD,i} = \tilde{\overline{q}}_{D,i} \left\{ \begin{array}{l} \dfrac{\pi}{a_{eD}} \left[\dfrac{\mathrm{ch}\left(\sqrt{f_f}\left(b_{eD} - \left|y_D + y_{wFD,i}\right|\right)\right) + \mathrm{ch}\left(\sqrt{f_f}\left(b_{eD} - \left|y_D + y_{wFD,i}\right|\right)\right)}{\sqrt{f_f}\,\mathrm{sh}\left(\sqrt{f_f} b_{eD}\right)} \right] + \\ \dfrac{1}{L_{HF,i}} \displaystyle\sum_{k=1}^{+\infty} \left[\dfrac{\mathrm{ch}\left(\varepsilon_k\left(b_{eD} - \left|y_D + y_{wFD,i}\right|\right)\right) + \mathrm{ch}\left(\varepsilon_k\left(b_{eD} - \left|y_D + y_{wFD,i}\right|\right)\right)}{\varepsilon_k \mathrm{sh}\left(\varepsilon_k b_{\mathrm{eD}}\right)} \times \right. \\ \left. \dfrac{1}{k} \sin\left(\dfrac{2k\pi L_{HFD,i}}{a_{eD}}\right) \cos\left(\dfrac{2k\pi x_D}{a_{eD}}\right) \cos\left(\dfrac{2k\pi x_{wFD,i}}{a_{eD}}\right) \right] \end{array} \right\} \tag{B-8}$$

where the $\varepsilon_k = \sqrt{f_f(s) + (k\pi/h_{fD})^2}$.

Under the assumptions of the FCR model given in Eqs.(4)~(5), it is more reasonable to represent the seepage equation for microfracture in IFNR using a Cartesian coordinate system. Based on the line source function method, the pressure solution for microfracture in INFR can be derived as follows:

$$\overline{m}_{fD} = \frac{\tilde{\overline{q}}_D}{2} \left\{ \begin{array}{l} \dfrac{\pi}{2} \left[\dfrac{\mathrm{ch}\left(\sqrt{f_f}\left(h'_{CD} - \left|\xi_{y,D} + \xi_{y,CD}\right|\right)\right) + \mathrm{ch}\left(\sqrt{f_f}\left(h'_{CD} - \left|\xi_{y,D} - \xi_{y,CD}\right|\right)\right)}{\sqrt{f_f}\,\mathrm{sh}\left(\sqrt{f_f} h'_{CD}\right)} \right] + \\ \displaystyle\sum_{k=1}^{+\infty} \left[\dfrac{\mathrm{ch}\left(\varepsilon_k\left(h'_{CD} - \left|\xi_{y,D} + \xi_{y,CD}\right|\right)\right) + \mathrm{ch}\left(\varepsilon_k\left(h'_{CD} - \left|\xi_{y,D} - \xi_{y,CD}\right|\right)\right)}{\varepsilon_k \mathrm{sh}\left(\varepsilon_k h'_{CD}\right)} \times \right. \\ \left. \dfrac{1}{k} \sin\left(\dfrac{k\pi}{2}\right) \cos\left(\dfrac{k\pi\xi_{x,D}}{L_{Fs,D}}\right) \cos\left(\dfrac{k\pi\xi_{x,CD}}{L_{Fs,D}}\right) \right] \end{array} \right\} \tag{B-9}$$

where in Eq.(B-8), $\xi_{x,D}$ and $\xi_{y,D}$ indicate the dimensionless vertical and parallel distance to the hydraulic fracture segment within the FCR region, respectively; $\xi_{x,CD}$ and $\xi_{y,CD}$ represent the coordinates of the midpoint of the fracture segment; and $L_{Fs,D}$ indicates the dimensionless length of the hydraulic fracture segment of one FCR region.

Appendix C. Derivation of the Seepage Equations of the HFN

The solutions of the HFN seepage equations

This calculation applies the method proposed by Cinco-Ley et al. (1981). solve the seepage equation of the discrete HFN model. According to Eq. (22) and the dimensionless parameter in Appendix A, the dimensionless seepage function of HFN can be written as follows:

$$\frac{\partial^2 \overline{m}_{FD}}{\partial \zeta_D^2} + \frac{2}{F_{CD}\zeta}\frac{\partial \overline{m}_{fD}}{\partial \delta_{fD}}\bigg|_{\delta_{fD}=w_{FD}/2} = 0 \tag{C-1}$$

The boundary condition of gas flow in HFN is as follows:

$$\frac{\partial^2 \overline{m}_{FD}}{\partial \zeta_D^2}\bigg|_{\zeta=0} = -\frac{4\pi}{F_{CD}}\overline{q}_{fD} \tag{C-2}$$

Under the assumption that the fracture tip is closed, the following is obtained:

$$\frac{\partial^2 \overline{m}_{FD}}{\partial \zeta_D^2}\bigg|_{\zeta\to \text{limit}} = 0 \tag{C-3}$$

According to the Cinco-Ley method, the following is obtained:

$$-\pi \overline{q}_{fD} = \frac{\partial \overline{m}_{fD}}{\partial \delta_{fD}}\bigg|_{\delta_{fD}=w_{FD}/2} \tag{C-4}$$

Then making use of Eqs. (C-1) and (C-4), the following equation is obtained:

$$\int_0^{\zeta_{\Omega D}}\int_0^{\theta_{\Omega D}} \frac{\partial^2 \overline{m}_{FD}}{\partial \zeta_D^2} d\theta_D d\zeta_D = \int_0^{\zeta_{\Omega D}}\int_0^{\theta_{\Omega D}} \overline{q}_{\Omega D,i} d\theta_D d\zeta_D \tag{C-5}$$

Finally, based on the discreteness of HFN rules, the Eq. (C-5) can be written as follows

$$\overline{m}_{\Omega D}(0) - \overline{m}_{\Omega D,i}(\zeta_{\Omega D}) = \frac{2\pi}{F_{CD,i}}\left[2\overline{q}_{\Omega D,i}\Delta l_{FD,i}\zeta_{\Omega D,i} - \int_0^{\zeta_{\Omega D}}\int_0^{\theta_{\Omega D}} \overline{q}_{\Omega D,i} d\theta_D d\zeta_D\right] \tag{C-6}$$

where $\overline{m}_{\Omega D}(0)$ indicates the pseudo-pressure of the wellbore; $\overline{m}_{\Omega D,i}(\zeta_{\Omega D})$ indicates the pseudo-pressure in the *i*-th segment of HFN.

The flow intersection relationship matrix

The flow relationship at the intersection of discrete fractures in Eq. (43) is represented using the connectivity matrices $\mathbf{C}_{SB}$ and $\mathbf{C}_{BH}$. For example, Fig. A1 shows a simplified fracture network, which is separated into six fracture segments (shown in Fig. A1 (b)). The direction of fluid flow within the fracture at the intersection of the

fractures is shown in Fig. A1 (c) and A1 (d). Thus, the flow rate convergence can be represented as follows:

$$\mathbf{C}_{SB}\mathbf{C}_{BH} = \begin{bmatrix} 1 & 0 & 0 & 0 & 0 & 0 \\ 0 & 1 & 0 & 0 & 0 & 0 \\ 0 & 0 & 1 & 0 & 1 & 1 \\ 0 & 0 & 0 & 1 & 0 & 0 \\ 0 & 0 & 0 & 0 & 1 & 0 \\ 0 & 0 & 0 & 0 & 0 & 1 \end{bmatrix} \begin{bmatrix} 1 & 0 & 1 & 1 & 0 & 0 \\ 0 & 1 & 0 & 0 & 0 & 0 \\ 0 & 0 & 1 & 0 & 0 & 0 \\ 0 & 0 & 0 & 1 & 0 & 0 \\ 0 & 0 & 0 & 0 & 1 & 0 \\ 0 & 0 & 0 & 0 & 0 & 1 \end{bmatrix} \tag{C-7}$$

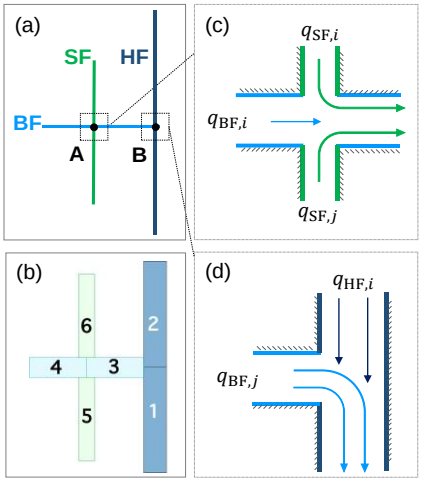

Fig. A1 Schematic of gas flow rate convergence of fracture network: (a) A case of fracture intersects; (b) form of discrete fracture element with the label of order; (c) fluid convergence between SF and BF at A-node; and (d) fluid

Appendix D. Sensitive analysis for model parameters

The type of hydraulic fractures of MFHW

In this section, three types of hydraulic fracture systems were categorized, ranging from simple to complex: the HF model, which considered only hydraulic fractures; the HF + BF model, which considered hydraulic fractures with branch fractures; and the HFN model. Fig. A2 shows the comparison of typical curve differences under various hydraulic fracture system types under the condition that other parameters of seepage model were set at the same values, which revealed that the more complex the type of hydraulic fracture was, the lower the typical curve position from the transitional flow stage to the linear flow stage would be, which indicated that a minor production pressure differential was required under the same production conditions. The reason for this phenomenon could be explained as follows: As the total length of the hydraulic fracture (as the main flow channel of the fluid in the ultra-low-permeability reservoir) increased, the contact area between the fracture and the reservoir also increased, thus making the reservoir fluids more easily exploited. In addition, from the biradial

stage, the m'_{wD}-t_D curve of the HFN model was higher than that of other hydraulic fracture types and reached the boundary control flow stage earlier.

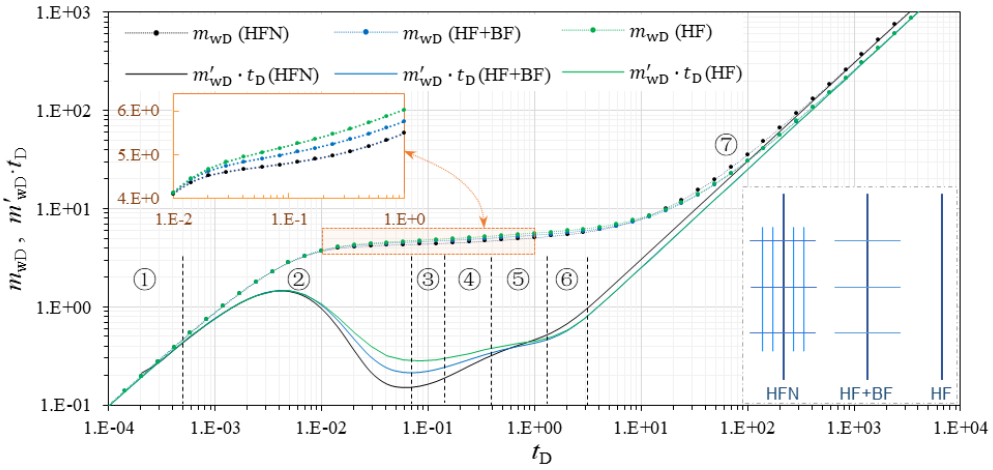

Fig. A2 Comparison of the typical curves under different hydraulic fracture types

Conductivity of hydraulic fractures

Eq. (A-5) shows that the value of k_{HF}, k_{mf}, w_F, and L_{HF} jointly determined the value of F_{CD}, and the individual changes of these parameters directly affected the value of F_{CD}. Thus, it was not conducive to clarify the direct influencing factors by comparing only the differences of typical curves with different F_{CD} values, which likely caused ambiguity in the interpretation of the model's parameter. Given this, the following parameter assignment was made to analyze the sensitivity of parameters relevant to F_{CD}: The change in the value of a relevant parameter of F_{CD} under the condition in which F_{CD} was equal to a specific value (as shown in Set 1 and Set 2 of Table A1. In addition, added a set of parameter values as shown in Set 3 of Table A1 was added to ensure that the ratio of k_{HF} to k_{mf} was constant. Then, the value of the two was changed in equal proportion, and the typical curve under each value scheme was drawn.

Table A1 parameters related to F_{CD}

Set 1	Constant: L_{HF}=80m; w_F=1×10^{-3}m; k_{mf}=2.50mD Variable: F_{CD}(k_{HF}=4000mD)=0.02, F_{CD}(k_{HF}=3000mD)=0.015, F_{CD}(k_{HF}=2000mD)=0.01
Set 2	Constant: L_{HF}=80m; w_F=1×10^{-3}m; k_{HF}=4000mD Variable: F_{CD}(k_{mf}=2.50mD)=0.02, F_{CD}(k_{mf}=3.33mD)=0.015, F_{CD}(k_{mf}=5.0mD)=0.01
Set 3	Constant: L_{HF}=80m; w_F=1×10^{-3}m; F_{CD}=0.02 Variable: F_{CD}(k_{HF}=4000mD,k_{mf}=2.5mD)=0.02, F_{CD}(k_{HF}=2000mD,k_{mf}=1.25mD)=0.02, F_{CD}(k_{HF}=1000mD,k_{mf}=0.625mD)=0.02

Compared with Fig. A3 and Fig. A4, when altering the values of k_{mf} and k_{HF} to decrease F_{CD}, the position of the typical curve was elevated, and the duration of the transition flow stage was extender. Regardless of the factors that led to a decrease in hydraulic fracture conductivity, it will result in a shorter duration of the bilinear

flow stage resulted. When the microfracture permeability increased, however, it led to a decrease in dimensionless conductivity (Fig. A4) Then, the duration of the formation flow stage remains almost unchanged, If the decrease in hydraulic fracture conductivity is due to a reduction in the microfracture permeability (Fig. A3), the duration of the linear flow stage in the reservoir would decrease, and more stages would be masked by the transient flow stage.

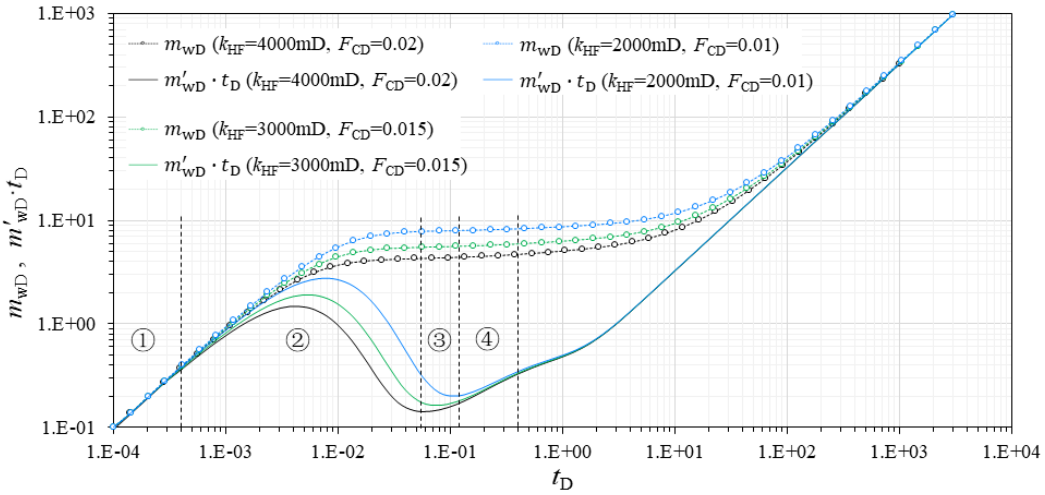

Fig. A3 Effect of k_{HF} on the typical curve under the value of Set 1 in Table. A1

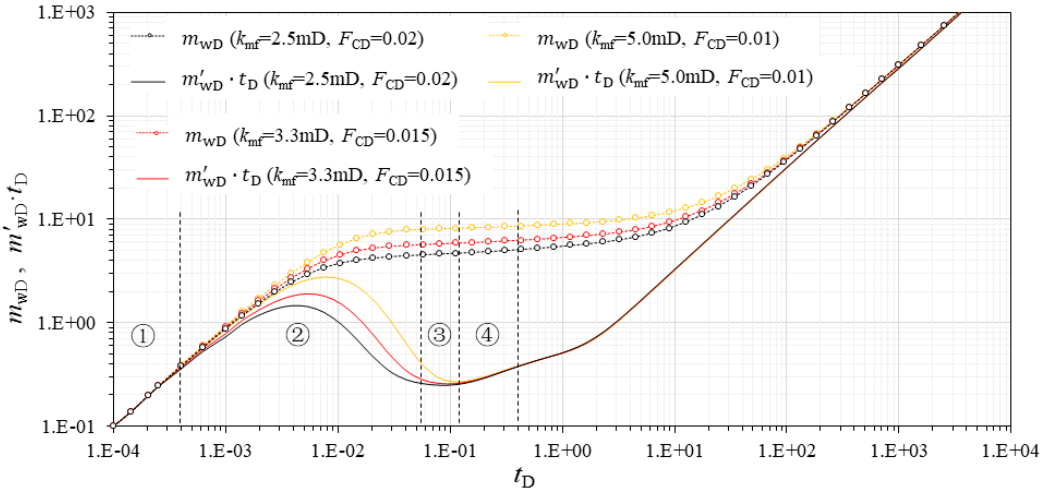

Fig. A4 Effect of k_{mf} on the typical curve under the value of Set 2 in Table. A1

Furthermore, in combination with Fig. A5, it was evident that if k_{HF} and k_{mf} increased with the same proportion (the F_{CD} decrease was constant), then the position of the typical curve would be lower, but it would coincide at the biradial flow stage. Given this finding, because the k_{HF} and k_{mf} had different influences on typical curves, in PTA, the direct assignment of combination parameters, such as F_{CD}, should be reduced. Thus, by individually analyzing the model parameters, to the degree possible, it may be possible to avoid some of the flow

laws from failing to be recognized.

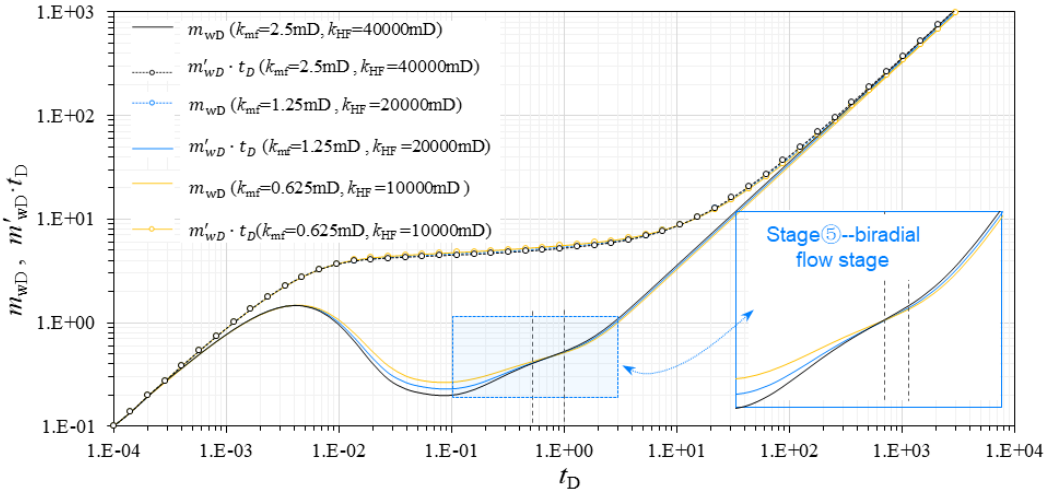

Fig. A5 Effect of k_{mf} and k_{HF} on the typical curve under the value of Set 3 in Table. A1